

Corrosion behavior of CuZnAl shape memory alloy in three different media.

Ekbal Mohammed Saeed¹, Zainab Hassan²

^{1,2}Metallurgical Engineering Department / collage of Materials Engineering / University of Babylon, Iraq

Mat.ekbal.moh@uobabylon.edu.iq

mmad92888@gmail.com

Abstract

Copper based shape memory Alloys are interesting group of metal alloys that have a widespread potential in medical and industrial applications. Cu-based shape memory alloys of Cu-22Zn-4Al alloy as master alloy have been prepared by powder metallurgy technique with and without the addition of (0.2 and 0.4) wt.% of Zr. After mixing the powders for 5hr, the alloys were prepared using 650MPa compact pressure. The alloys were subjected to sintering process in vacuum tube furnace with three steps. Several tests such as microstructures observation and phase analysis using scanning electron microscope, and X-ray diffraction analysis have been done. Electrochemical corrosion tests for alloys with and without the addition of (Zr) was carried out using potentiodynamic polarization technique in three different solutions (HCl, NaOH, NaCl). XRD and microstructural analysis showed that all alloys compositions consisted of the predominating Cu₅Zn₈ phase. Corrosion test results have showed that the highest corrosion resistance was found in the addition of (0.4 wt.% Zr) which give the lowest corrosion rate (30.31mpy) in 3.5% NaCl solution. Noted that the corrosion rate of base alloy was (86.88)mpy

Keywords: Cu-Zn-Al alloy; Corrosion, Powder Metallurgy; Microstructure, Zirconium.

1. Introduction .

SMA's are an important class of smart materials able to recover after deformation a pre-imposed shape through a temperature modification. These alloys show great potential, finding several applications in medicine and indifferent types of industry sectors (aerospace, architecture, automotive etc.) [1]. The copper-based shape memory alloys are easy to fabricate mostly, their process are less expensive when compared to (Ni-Ti) shape memory alloys. However, in the polycrystalline state (Cu-Al-Ni) and (Cu-Zn-Al) shape memory alloys are brittle for this reason cannot be easily worked due to the high degree of order and high elastic anisotropy of the parent β -phase (austenitic) [2]. Copper-based shape memory alloys can be strained up to (4-5%), and then convert to its primary shape [2]. The commercial Availability for the transformation temperature ranges between (-180 and +200 C (copper-zinc-aluminum) alloy [3]. Cu-Zn-Al alloys Compositions usually fall in the range of (15-40 wt% Zn) and (4-8 wt.% Al). The martensitic transformation temperatures can be adjusted by varying chemical composition [4]. In different practical applications, when the alloys are exposed to different corrosive media for a longer time they are displayed to corrosion and pitting. Therefore, study of corrosion potential and pitting potential of the alloys are very necessary before they are put into biomedical and

industrial applications. It was observed that corrosion rate of austenite was more than martensite in Cu-Al-Ni SMAs. It was detected that for the sample in the austenitic structure the current density is greater than for martensitic structure. This proves the corrosion resistance for the shape memory alloys is more than other traditional alloys because of the hyperactive elastic behavior of polycrystalline structure [5]. In (2013) Sathish et al [6], Four shape memory alloys of Cu-Zn-Ni, in the range of 35-55 wt% of Cu, 43-60 wt% Zn and 2-9 wt% Ni, were prepared by ingot metallurgy route in an induction furnace under an inert atmosphere. The shape memory effect was tested by bend test. The alloys were further tested for their corrosion behavior in fresh water, Hank's solution and sea water. From the results it was observed that the alloys exhibit high corrosion resistance in fresh water when compared to Hank's solution and sea water. And it was also observed that the alloys exhibit better corrosion resistance in Hank's solution than in sea water. In (2014) Jassim Mohammed et al. [7], studied the corrosion behavior of (CuAlZn) Shape Memory Alloys in (3.5 NaCl) Solution, The rate of corrosion for sample in austenitic structure is much superior than for martensitic structure. Corrosion rate for alloys was decreased with increasing the percent of alloying elements (Mn, Ti). Among the alloys, quenched alloy (Cu-25Zn-4Al-1%Ti) has less corrosion rate. The aim of this research is to prepare Cu Zn Al shape memory alloy specimens by using powder metallurgy technique, study the corrosion rate in different solutions HCl, NaOH, and 3.5% NaCl and microstructure after corrosion.

2. Experimental Work.

2.1. Materials.

In this work, Powders of Copper (Cu), Zinc (Zn), Aluminum (Al) and Zirconium (Zr) of 99.9% purity were used as raw materials to prepare the alloy specimens of the present study. The particle size of the powders was analyzed via (the better size 2000, laser particle size analyzer). Table 1 shows the particle size and the supplier of each powder.

Table 1. The particle size and the supplier of the used powders

Material (Powder)	Average particle size (μm)	Source
Cu	54.14	Changsha Xinkang Advanced Material Co., Ltd
Zn	16.49	Changsha Xinkang Advanced Material Co., Ltd.
Al	18.66	Changsha Xinkang Advanced Material Co., Ltd.
Zr	6.162	Changsha Xinkang Advanced Material Co., Ltd.

In the process of manufacturing the specimens using powder metallurgy, Cu-22%Zn-4%Al-XZr ($x=0.2\%$, 0.4%), is the primary mixture utilized. After that, the weighted

powder combination was mixed for five hours in order to obtain a fine and consistent dispersion of particles powder. The compact pressure was found to be 650 MPa. After that, the material was sintered in inert gas (argon) for one hour at 350 °C, then for one hour at 550 °C, and for two hours at 850 °C. The specimens were then allowed to cool to room temperature in the furnace. All specimens underwent a one-hour quenching heat treatment at 850°C to stabilise the β -phase structure. Following this, they underwent rapid cooling by submerging in 20°C cold water. **Table (2)** provides details on the specimen code and composition used in this experiment.

Table 2. prepared specimens in the present study.

Alloy Code	Chemical Composition (wt) %
(base)	Cu-22%Zn-4%Al
A	Cu-22%Zn-4%Al-0.2%Zr
B	Cu-22%Zn-4%Al-0.4%Zr

2.2 Materials Characterization.

SiC paper grits sized (250, 400, 600, 800, 1000, 1200, 1500, and 2000) used in the wet grinding and polished with diamond paste; and etched in a room-temperature solution of (10 mLHCl+5 gFeCl₃+H₂O) according to **ASTM E407 - 07[8]**. The specimen was washed and dried using distilled water and an electric dryer following etching. A light optical microscope of the Belphoptic type was used to view and study the specimens' microstructure, and a TESCAN VEGA3, USA scanning electron microscope (SEM) was used to look at the samples' microstructure up close. We used an X-ray diffract meter (XRD) (model: SHIMADZU Lab XRD-6000) to study the base's phases. In the XRD studies, CuK α radiation operating at 40 KV and 7 mA was used as the X-ray source. The samples were scanned in a θ range from 30 to 80.

2.3 Corrosion Test.

The corrosion test was done by using the potentiodynamics polarization test in three different solutions: acid solution(HCl) ,basic solution(NaOH) and (3.5gm NaCl +96.5ml distilled water), for all specimens with and without additives, the test was conducted at room temperature (25 °C). A platinum wire was used as counter-electrode, the working electrodes were made of cylindrical pieces fastened with appropriate nut and reference electrode. The process has been programmed in computer to draw potential(mv) and log current (μ Am) to obtain corrosion current by intersection of the tangents to the two curves . After that take SEMimage for more corrosive specimens and Optical microstructure for all specimens. Corrosion rate determined in electrochemical method by (corrosion current density) to expression by the equation (1) [9]

$$C.R(\text{mpy})= 0.13 * i_{\text{corr.}} * \frac{e}{\rho} \quad \dots\dots\dots(1)$$

$i_{\text{corr.}}$ =corrosion current density in (Amp/cm²) .

e = weight chemical equivalent for metal

Where :

mpy=mil per year

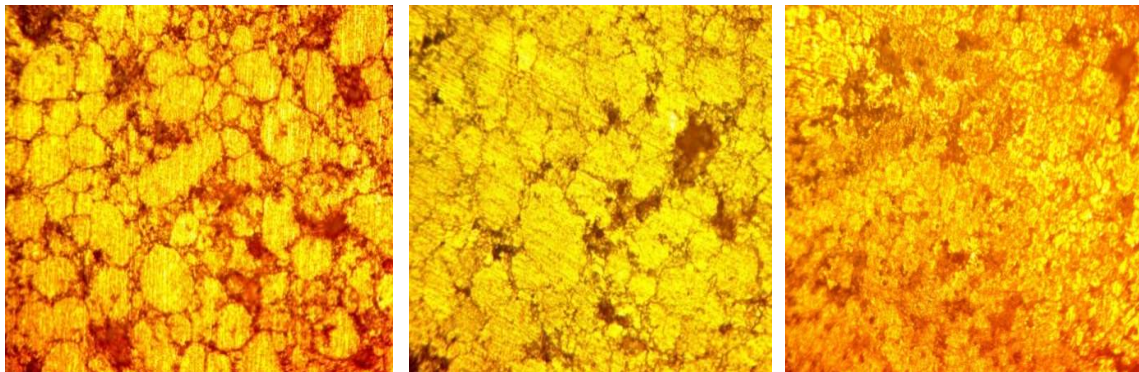
$$e = \frac{\text{atomicweight}}{\text{equivalent}}$$

ρ = theoretical density in (g/cm³).

3. Results and discussions.

3.1 Microstructural characteristic of Cu-Zn-Al.

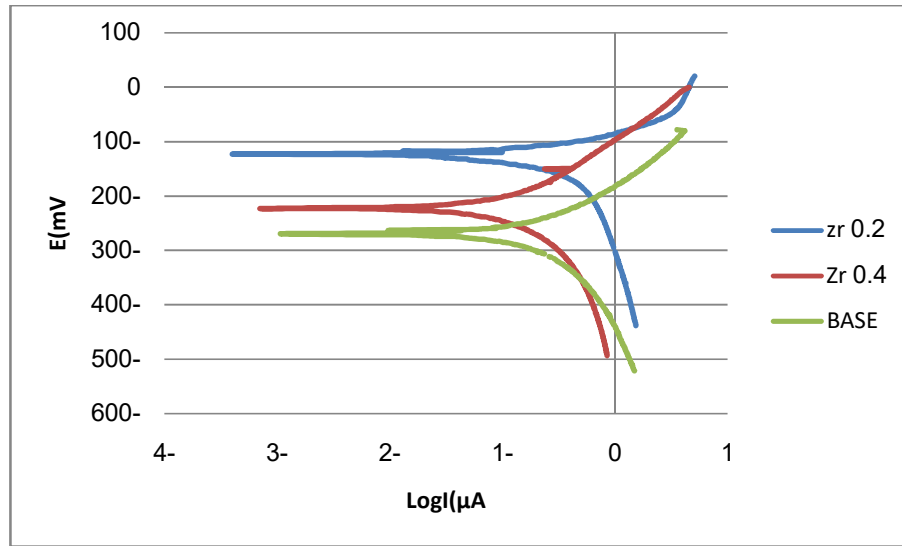
Fig. (1a) shows the microstructure of tested alloy, where a relative coarse grain structure can be observed. this is expect, because it represents one of the characteristic of this alloy without any improvements or additions which have a significant impact on the properties while in figure (1 b,c) . the grain became fine with (0.2%)Zr alloying element addition and became finer when percentage of Zr reach (0.4%) respectively.From the figure below, there are two phases.the first phase is Zn-rich phase (dark area on grain boundary) and Zn-poor phase (bright area on grain boundary), the phase refer to β and α phases respectively.



Figure(1)Optical Microscope Image(20X): (a) for Sintered base Alloy, (b) for Sintered Alloy with wt. 0.2% Zr (c) for Sintered Alloy with 0.4% Zr.

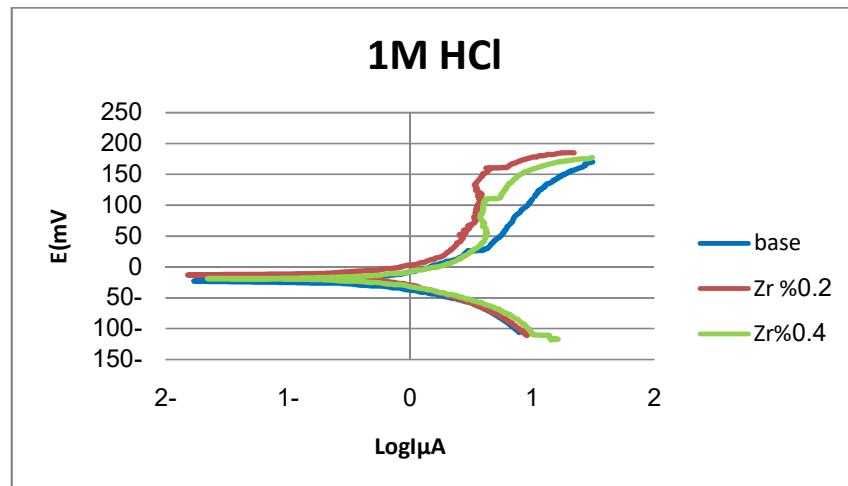
In figure (2 a,b),X-ray diffraction tests were done for all specimens after the sintering. The phases produced as a result of sintering process can be seen in figure (2a),(2b). From the figure(2a)for base alloy we can see all phases appeared for this alloy:Cu₅Zn₈intermetallic compound(quenching mainly produces β phase),AlCu (γ -cubic phase),Cu₉Al₄(γ_2 -solid solution),CuAl₂(tetragonal superstructure) and Cu,Zn pure peaks [10].All phases appear at (3-5) position in X-ray chart.while figure (2b)after adding (0.4%) XRD diffraction for B alloy show no different in results expect (Zn₂Zr₃) appear (intermetallic compound)[11].this intermetallic compoundeffective strengthening phases.

potential for oxidation and decrease current density is explained by formation (CuCl), (Cu₂O) and aluminum oxide [13].as a shown in figure (4).

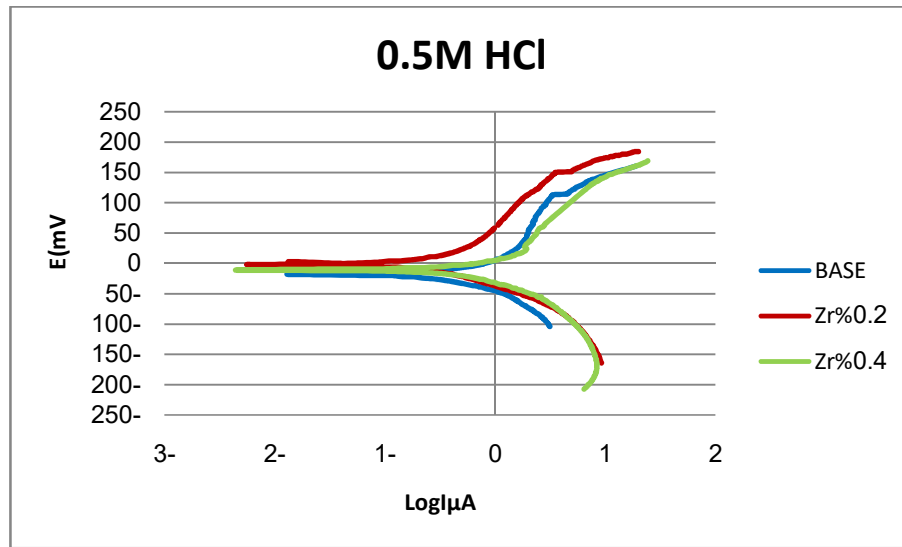


Figure(4): Potentiodynamic Polarization curve in 3.5% NaCl solution

Figures (5) and (6) depict the corrosion behavior and rate of all specimens in various concentrations (HCl) medium. This graphic indicates that the corrosion rate of base alloy increased with increasing concentrations of HCl reached to (507.16) mpy in 1M HCl while in 0.5M HCl corrosion rate reached to (383.46) mpy as shown in table (3). This is due to the more concentration of Cl⁻ ions in the solution of which causes more corrosion [140]. For specimen (B), we say previously this alloy has the best corrosion resistance compared to other alloys in (1M and 0.5M) HCl reached to (361.9 and 315.2) mpy respectively. While specimen (A) corrosion rate in (1M and 0.5M) is (370.73 and 331.53) mpy. Figure (7) and (8) image for surface specimens after corrosion test in (1M and 0.5M) HCl.



Figure(4): Potentiodynamic Polarization curve in 3.5% NaCl solution



Figure(4): Potentiodynamic Polarization curve in 3.5% NaCl solution

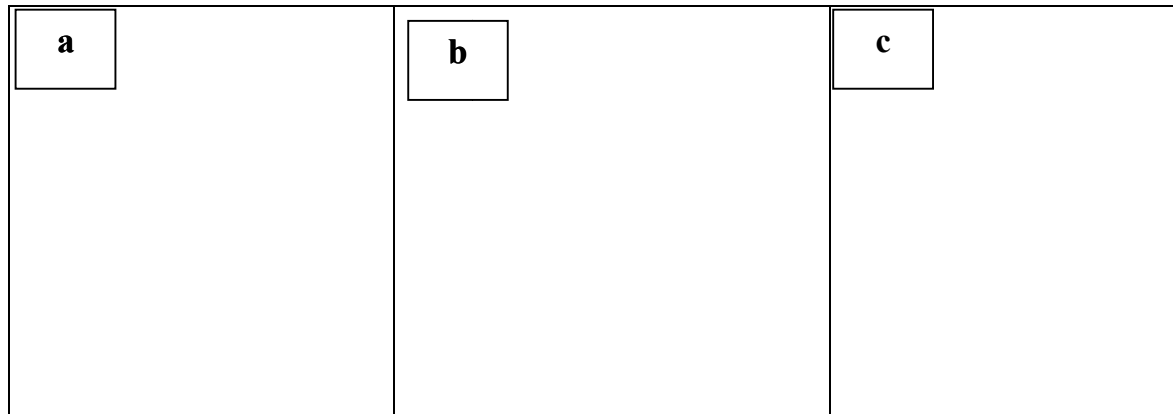


Figure (7): Microstructure after corrosion for all alloys in 1M HCl(20X) (a) base alloy (b) A alloy (c) B alloy .

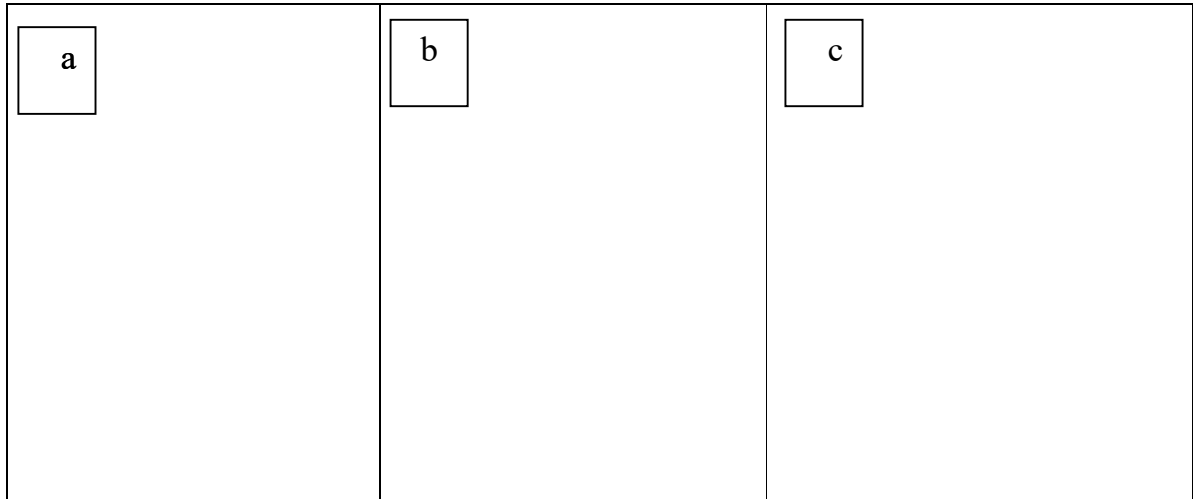
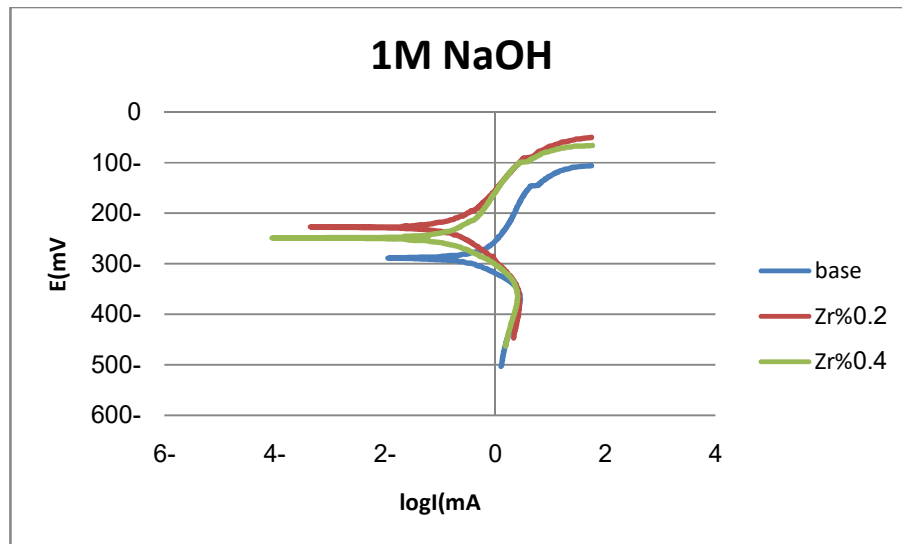


Figure (8):Microstructure after corrosion for all alloys in 0.5 M HCl(20X) (a) base alloy (b) A alloy (c)B alloy .

Figure(9) depicts corrosion behavior and rate of all specimens in (NaOH) media. As previously stated, alloy (B) has the best corrosion resistance among all specimens when compared to other alloys. The corrosion rate for this alloy reached to (65.65) mpy as shown in table (3).This reveals that shape memory alloys have higher resistance to corrosion than traditional alloys due to the hyper elastic behavior of their polycrystalline structures. It's likely that phase transformation-induced structural ordering influences the corrosion behavior for CuZnAl shape memory alloys,[14].



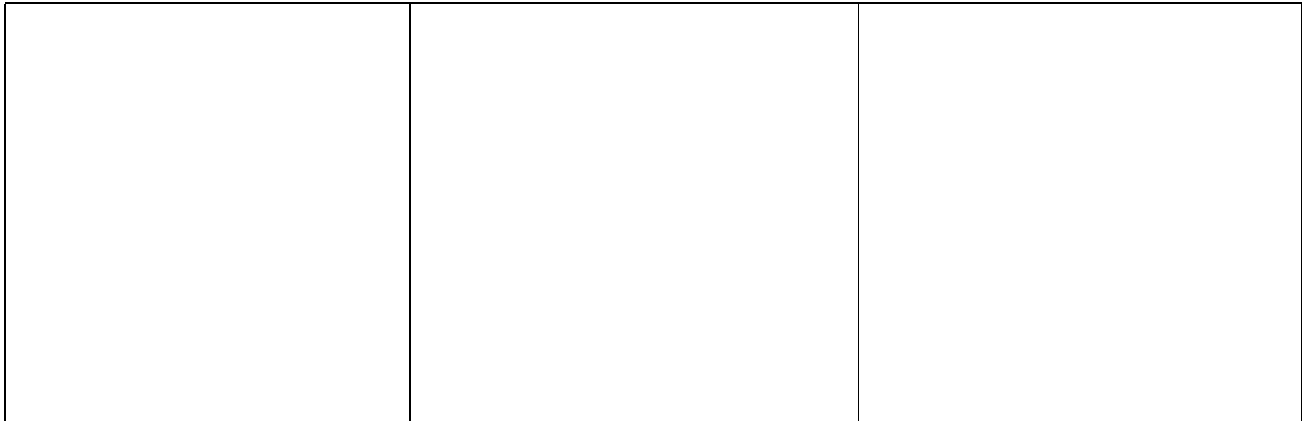
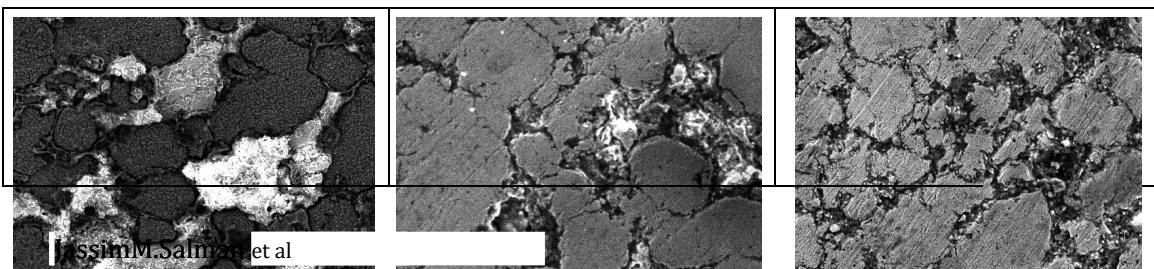


Figure (9):Microstructure after corrosion for all alloys in 1 M NaOH(20X) (a) base alloy (b) A alloy (c)B alloy .

Table (4.6): The Cu-Zn-Al SMA polarization characteristics in three distinct corrosion solutions with and without Zr addition.

Alloy code	Corrosion solution	E _{corr} (mV)	I _{corr} (μ A/cm ²)	Corrosion Rate (mpy)
Base	3.5% NaCl	-152.3	126.71	86.88
A		-124.3	56.59	38.80
B		-220.8	44.21	30.31
Base	1M HCl	-22.2	739.6	507.16
A		-12.9	540.7	370.73
B		-19.7	527.8	361.9
Base	0.5M HCl	-20	559.26	383.46
A		4.2	483.53	331.53
B		-10	459.79	315.2
Base	1M NaOH	-288.1	543.12	372.40
A		-225	117.95	80.86
B		-247.4	95.67	65.56

Figures(10 and 11) illustrates SEM image confirm the optical microstructure image for more corrosive specimens in three different media,It insures the successof the manufacturing process and appearance ofmartensite phases in the form of layers and α alphaphase it appear in the bright regions whiledark regions it refers to the beta phase β . Themicrostructure includes some of pores, and thepercent of these pores affect the alloy density asmentioned in section of porosity the specimens .



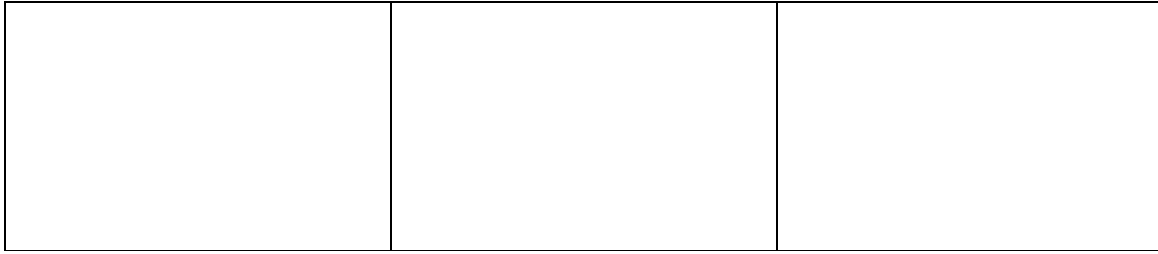


Figure (10):SEM for base alloy(50X) in (a) 1M HCl (b) 0.5M HCl(c)NaOH

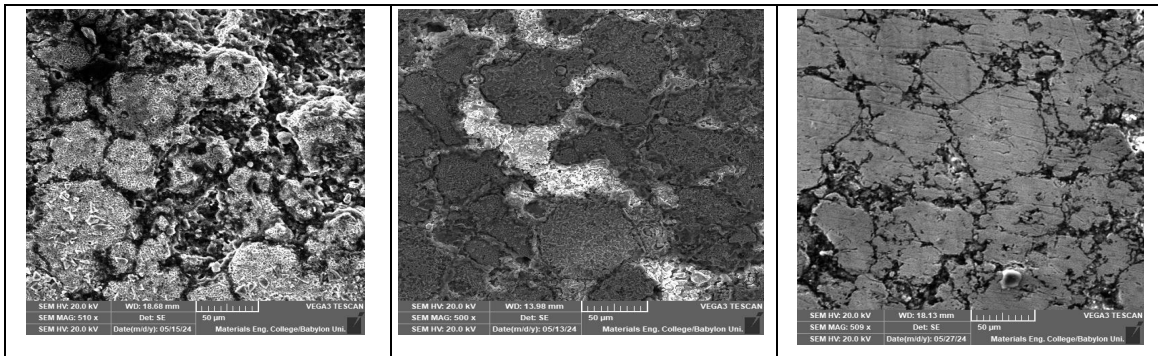


Figure (11):SEM for A alloy(50X) in (a) 1M HCl (b) 0.5M HCl(c)NaOH

Conclusion.

From studying the investigation of corrosion behavior of copper-based shape memory alloy in different media all the specimens with and without additives consist of two main phases (β -phase) and (α -phase), this is obtained from XRD and microstructure Observations. The corrosion rate decreases with increase in Zr percentage in all solutions (HCl, NaOH and NaCl) the perfect addition was 0.4% Zr element because have the lower corrosion rate in all solutions.

Reference.

- [1] Brotzu, A., De Filippo, B., Natali, S., & Zortea, L. (2022). Corrosion behavior of Shape Memory Alloy in NaCl environment and deformation recovery maintenance in Cu-Zn-Al system. *FRATTURA E INTEGRITÀ STRUTTURALE*, 16(62), 64-74.
- [2]. T. Lenau "Shape Memory Applications Inc.," Nitinol Devices & Components Inc. 2003. Available: <http://www.designinsite.dk/htmsider/m0173.htm> .
- [3]. Sutou, Y., Omori, T., Kainuma, R., Ishida, K., & Ono, N. (2002). Enhancement of superelasticity in Cu-Al-Mn-Ni shape-memory alloys by texture control. *Metallurgical and Materials Transactions A*, 33, 2817-2824.
- [4]. Davis, J. R. (Ed.). (2001). *Copper and copper alloys*. ASM international.

- [5] Ali, A. R. K. A., & Al-Tai, Z. T. K. (2010). The effect of iron addition on the dry sliding wear and corrosion behavior of Cu Al Ni shape memory alloy. *Eng. Technol. J*, 28, 6888-6902.
- [6] Sathish, S., Mallik, U. S., & Raju, T. N. (2013). Corrosion behavior of Cu-Zn-Ni shape memory alloys.
- [7] Jassim Mohammed Salman, Abdul Raheem K. Abid Ali and Huda Abbas Kheralla, "Corrosion study of CuAlZn Shape Memory Alloys in 3.5 NaCl Solution", Materials Engineering College, Babylon University, Iraq, 2014.
- [8] STM E407 - 07 (2011) " Standard Practice for Microetching Metals and Alloys" ASTM international .
- [9] Annual Book of ASTM standards, Wear and erosion, Metal corrosion, American Society for Testing and Materials, Vol. 03. 02, G5 -87, 1988.
- [10] Kwarciak, J.: Phase transformations in Cu-Al and Cu-Zn-Al alloys. *J. Thermal Anal. Calorim.* **31**(3), 559-566 (1986).
- [11] Wang, S., Zhao, Y., Guo, H., Lan, F., & Hou, H. (2018), 'Mechanical and thermal conductivity properties of enhanced phases in Mg-Zn-Zr system from first principles', *Materials*, 11(10), 2010.
- [12] A. H. Haleem, Z. T. Khulief, and I. N. Kadhim, "Modification of Corrosion and Mechanical Behaviour of Cu-Zn-Al Shape Memory Alloy," in *Journal of Physics: Conference Series*, IOP Publishing, 2021, p. 12049.
- [13] M. Gojic , L. Vrsalovi , S. Kozuh , A. Kneissl , L. Anzel , S Gudi , B. kosec , and M. kliski , Electrochemical and microstructure study of Cu-Al-Ni shape memory alloy , adopted from *Journal of alloy and compound* , 2011, 9782-9790.
- [14] Abdul Raheem K. Abid Ali and Zuheir T. Khulief Al-Tai, "The Effect of Iron Addition on the Dry Sliding Wear and Corrosion Behavior of Cu Al Ni Shape Memory Alloy," *Engineering and Technology Journal*, Vol. 28, No. 24, 2010, pp. 6888-6902.